Optimization and experimental study of the auxiliary mechanism for organic fertilizer side throwing

Hongxin Liu[1], Yongtao Xie[1,2*], Yijian Zhao[2], Jiajie Shang[2]

(1. *College of Mechanical and Electrical Engineering, Suqian University, Suqian 223800, China*;
2. *College of Engineering, Northeast Agricultural University, Harbin 150030, China*)

Abstract: To correct the working state of a throwing component and achieve an ideal narrow, far, and uniform material projectile flow for a side-throwing device for organic fertilizer with inclined opposing discs, a systematic optimization of the auxiliary mechanisms (baffle, upper deflector, and side deflector) was performed. Starting from a basic analysis of the working principles of each side-throwing device component, theoretical modeling and MATLAB numerical calculations were used to determine the departure angle providing the farthest fertilizer distance, as well as the maximum and minimum throwing angles required to achieve a target distance of 10 m. These calculations informed the optimization and configuration of the basic structures of each auxiliary mechanism component. The impact of the baffle on fertilizer movement was analyzed, leading to an optimization of the baffle's height and its horizontal position in relation to the main throwing disc, guiding the design of the discharge port structure. Combining the theoretical analysis results, the surface of the upper deflector was fitted, and a side deflector was added to assist in limiting the scattering angle of the projectile flow. An EDEM simulation showed that the optimized auxiliary mechanisms worked well together, resulting in a narrower discharge width, a more concentrated projectile flow, and improved uniformity in spreading. Prototype testing confirmed that from the side projection angle between the spreading direction and vertically upward, the projectile flow angle domain was adjusted from 18°-45° to 23°-32°. With the optimization of other auxiliary mechanisms, the coefficient of variation in spreading uniformity decreased from 25.95% to 19.21%, the effective throwing distance increased from 10.1 to 11.2 m, and the scattering angle decreased from 12° to 4°, effectively enhancing the performance of the side-throwing device.

Keywords: organic fertilizer side throwing, auxiliary mechanism, optimization research, virtual simulation, experiment
DOI: 10.25165/j.ijabe.20251804.9168

Citation: Liu H X, Xie Y T, Zhao Y J, Shang J J. Optimization and experimental study of the auxiliary mechanism for organic fertilizer side throwing. Int J Agric & Biol Eng, 2025; 18(4): 157–169.

1 Introduction

In recent years, China's national agricultural strategy has been adapted to achieve green, organic, ecological, and sustainable objectives. The replacement of chemical fertilizers with organic fertilizers has gradually become an inevitable choice in sustainable agriculture. With abundant raw materials and mature processing technology, organic fertilizers, when applied over the long term, can significantly improve the physical and chemical properties of soil and enhance its fertility[1-3] Additionally, the raw materials of organic fertilizer can pollute the environment and are difficult to dispose of, and turning this liability into an asset solves several problems[4]. Among the equipment used for spreading organic fertilizers, side-discharge spreaders have attracted attention due to their ability to perform as well as rear-discharge spreaders while providing the advantages of longer throwing distances, less susceptibility to wind, and adaptability to various terrain conditions. However, the existing limited number of side-discharge spreaders is restricted by their basic structures and working principles, low reliability, poor adaptability to materials, and limited discharge capacity with a small adjustment range. Furthermore, they require specially designed feeding devices, which lack universality and have complex structures and high supporting costs, resulting in very low production and sales of these implements.

To this end, we innovatively developed an organic fertilizer side throw device with inclined opposing discs. The fertilizer is thrown sideways in the forward direction of the implement. We conducted in-depth research on the main throwing inclined opposing discs and an assisting roller, which achieved good basic main throwing flow[5,6]. However, due to its special inclined forward throwing working principle and the narrow, distant, and uniform requirements of the sideways throwing flow shape, the organic fertilizer material flow undergoes multiple corrections and adjustments in direction and path during the throwing process. Therefore, auxiliary mechanisms such as baffle plates and flow deflectors need to be configured to perform multiple corrections on the basis of the main throwing flow to achieve a narrow, distant, and uniform target state.

As an important component of the organic fertilizer spreading device, the auxiliary mechanism has attracted the attention of scholars at home and abroad. The following is a review and analysis of the research on the auxiliary mechanism of the organic fertilizer spreading device by domestic and foreign scholars in recent years. For example, the French company KUHN effectively controlled the throwing angle of fertilizer particles and increased the throwing distance by developing and installing a guide plate for its

Received date: 2024-06-22 **Accepted date:** 2025-04-30
Biographies: **Hongxin Liu**, Professor, PhD, research interest: agricultural mechanization technology and equipment, Email: lcc98@163.com; **Yijian Zhao**, PhD candidate, research interest: organic fertilizer throwing technology and equipment, Email: zhaoyj5255@163.com; **Jiajie Shang**, PhD, Engineer, research interest: agricultural mechanization technology and equipment, Email: jazzy_shang@neau.edu.cn.

***Corresponding author: Yongtao Xie**, PhD candidate, research interest: organic fertilizer spreading mechanization technology and equipment. Northeast Agricultural University, Harbin 150030, China. Tel: +86-18678698606, Email: 18678698606@163.com.

independently developed hammer-type organic fertilizer side-throwing machine. Zhang et al.[7] reduced the velocity loss of fertilizer particles colliding with the baffle by designing and adding a cover plate and a diversion cover to the centrifugal side-throwing fertilizer spreader for lotus root fields. Fan et al.[8] studied the influence of the gap between the baffle plate and the blade on the distribution law of fertilizer particles thrown by the centrifugal organic fertilizer side-throwing device. The research results show that the throwing uniformity can be effectively improved by optimizing the gap between the baffle plate and the blade. Bing et al.[9] studied the action relationship between the auxiliary mechanism and the throwing disc, and effectively improved the crushing rate and throwing effect of organic fertilizer particles. V. Bulgakov et al.[10] increased the throwing efficiency by designing and installing a guiding device for the centrifugal fertilizer spreader to make the fertilizer fall into the high-speed throwing area of the disc. Zhou et al.[11] optimized the fertilizer deflector of a corn fertilization device; by analyzing the forces exerted on the fertilizer granules on the deflector, they determined parameters such as its bending angle and distances from other components so that the fertilizer could be distributed in different areas according to predetermined proportions, thus achieving accurate fertilization.

In summary, when studying baffle plates and deflectors, it is advisable to follow material movement patterns, fully consider the coordination between the material and relevant components, and utilize methods such as kinematic and dynamic analysis, virtual simulation, and experimentation to quantitatively explore the influence of structural parameters on material movement. This study focused on the core components of a side throw device with inclined opposing discs to conduct in-depth research on the auxiliary mechanisms, clarify the roles, and systematically optimize the structure and parameters in terms of correcting and adjusting the fertilizer's transfer, blockage, and motion path. The goal was to explore a theoretical approach for controlling and correcting the shape of solid material throwing flow patterns and provide practical examples for reference.

2 Main structure and working principle of the side throw device

2.1 Organic fertilizer side throw device with inclined opposing discs

The main components of the organic fertilizer side throw device with inclined opposing discs (hereinafter referred to as the side throw device) are shown in Figure 1 and mainly consist of fertilizer spreading discs with fertilizer scraper plates, an assisting roller, and auxiliary mechanisms (upper deflectors, side deflectors, and baffle plates). Fertilizer discs with scraper plates are the main throwing component of the side throw device and are responsible for the main task of spreading fertilizer. Its main technical parameters are listed in Table 1[5].

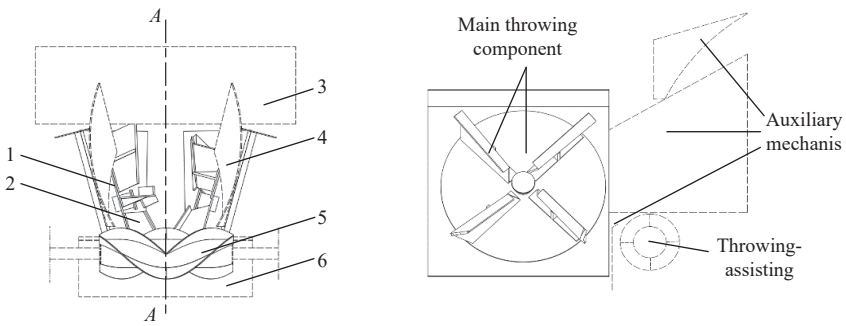

a. Front view b. A-A section view

1. Fertilizer spreading disc; 2. Fertilizer scraper; 3. Upper deflector; 4. Side deflector; 5. Assisting roller; 6. Baffle plate

Figure 1 Structural diagrams of the side throw device

Table 1 Main technical parameters of the main throwing component

Parameter	Value
Disc diameter/mm	500
Disc inclination angle (the angle between the disc and its projection on the horizontal plane)/(°)	75
Distance between the centers of the two discs/mm	320
Disc rotation velocity/r·min^{-1}	700

2.2 Functions and principles of the auxiliary mechanism

2.2.1 Baffle plate

(1) Control and blockage of fertilizer

During side throw device operation, the envelope swept out after one rotation of the inclined opposing discs with scraper plates consists of two inclined opposing cones. There is a certain gap between the bottom end of the cones and the device base plate. When the fertilizer continuously falls from the front hopper into the side throw device, a small portion will directly fall onto the base plate, while a portion of the remaining fertilizer carried by the scraper plate will also fall onto the base plate due to its carry-back effect. Fertilizer gradually accumulates in the gap, and when the fertilizer accumulates to the contact range of the scraper plate, the scraper plate will push out all the fertilizer within its operating range from the side throw device. Due to the slow pushing velocity, the weak ability of fertilizer to move farther away, and the short throwing distance, fertilizer accumulates near the device.

The baffle plate plays a role in controlling and blocking fertilizer in the gap. After the baffle plate is installed, the fertilizer is thrown at a certain angle (the angle between the direction of the fertilizer throwing velocity and the horizontal plane when a two-dimensional plane is established between the fertilizer throwing direction and the upward direction perpendicular to the ground). The ability of this part of the fertilizer to move farther is enhanced, and the throwing distance increases at the same time. In addition, fertilizer with a low initial velocity and an angle between the velocity and the horizontal plane less than the minimum departure angle is blocked inside the device.

(2) Working with the scraper plate to form a flexible cylinder cavity

When the bottom fertilizer is blocked, the baffle plate and the scraper plate work together to form a flexible cylinder cavity with a shape that can roughly match that of the envelope, as shown in

Figure 2. The space between the flexible cylinder cavity and the scraper plate can accommodate hard impurities, which act as a buffer to effectively prevent hard objects from damaging the device. Most of the fertilizer scraped by the scraper plate every time it sweeps across the flexible cylinder cavity accumulates at the end of the scraper plate (the area with the highest linear velocity on the scraper plate). The initial velocity and throw distance of this part of the fertilizer after being thrown are effectively increased.

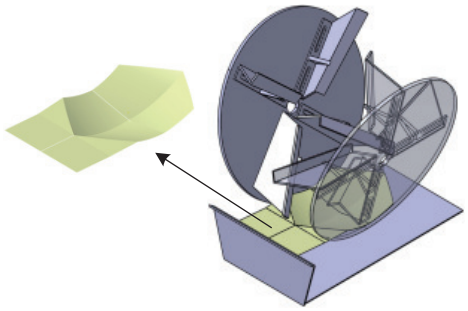

Figure 2 Schematic diagram of the flexible cylinder cavity

(3) Transferring the fertilizer to the throwing-assisting roller

The baffle plate has a certain height. The fertilizer thrown by the scraper plate at the smallest angle along the upper edge of the baffle plate is transferred to the working area of the assisting roller through the baffle plate structure; thus, the roller is used to solve the problem of fertilizer accumulation in the vicinity.

2.2.2 Upper deflector

This component is critical for increasing the fertilizer throwing distance and can limit part of the fertilizer throwing flow with an excessively large departure angle.

When the fertilizer leaves the scraper plate, it undergoes an oblique throwing motion in the air. During this process, the air resistance needs to be continuously overcome. Assuming that the mechanical energy of the fertilizer is constant, when the ascent height of the fertilizer exceeds the critical value that supports the fertilizer to reach the farthest distance, the greater the ascent height is, the greater the loss of mechanical energy caused by the additional work done to overcome air resistance, and consequently, the farthest distance the fertilizer can advance decreases accordingly. The ascent height of the fertilizer is determined by the departure angle of the fertilizer, so it is necessary to correct and adjust the trajectory of the fertilizer with excessively large departure angles using the upper deflector. Thus, after the limiting action of the upper deflector, an excessive increase in the height of the fertilizer can be prevented, thereby reducing the mechanical energy dissipation and increasing the effective throwing distance.

2.2.3 Side deflectors

When spreading fertilizer, in the fertilizer throwing flow with a smaller scattering angle (when fertilizer is spread by the side throw device in a stationary manner, the coverage area formed by the fertilizer after it lands is roughly an isosceles trapezoid, and the angle between the two sides of the trapezoid is defined as the scattering angle), most of the fertilizer moves together, while in the throwing flow with larger scattering angles, there will be individual fertilizer granules or small clusters of fertilizer moving independently. The former generally enhances the ability to resist air resistance compared to the latter as a whole, reducing the mechanical energy dissipated by the fertilizer due to movement to both sides. This part of the mechanical energy can be used for the longer distance movement of the fertilizer along the spreading direction. Therefore, to reduce the dissipation of mechanical energy, it is necessary to install side deflectors on the device to limit fertilizer with large scattering angles.

2.3 Analysis of the auxiliary mechanism contents

2.3.1 Baffle plate

(1) Coordination with the main throwing component

There is a large gap between the side of the flexible cylinder cavity close to the baffle plate and the envelope swept out by the scraper plate after one rotation. When the scraper plate scrapes the fertilizer from the side of the flexible cylinder cavity away from the baffle plate to the gap area, the end of the scraper plate no longer touches the flexible cylinder cavity. As a result, the fertilizer starts to fall off the end of the scraper plate. The velocity of the fertilizer that falls (separate from the scraper plate) decreases significantly, and the fertilizer cannot be replenished from the flexible cylinder cavity. As a result, the amount of fertilizer in the area on the scraper plate with the maximum linear velocity decreases. Together, these two factors lead to a reduction in the proportion of fertilizer applied at long throwing distances and a decrease in the overall effective throwing distance of the fertilizer.

One of the functions of the baffle plate is to limit the fertilizer with a small departure angle, that is, to block the part of the fertilizer in the device that has such a small initial velocity that it will fall to the nearby area after being thrown. However, the critical value for the small departure angle is unknown, which leads to an unclear and uncertain control effect of the baffle plate structure on fertilizer with a small departure angle.

(2) Coordination with the assisting component

In the process of moving the fertilizer to the assisting roller via the baffle plate, part of the fertilizer leaks from the gap between the upper edge of the baffle plate and the assisting roller and falls to the ground, causing some fertilizer to accumulate nearby and decreasing the throwing uniformity. The assisting roller impedes the movement of fertilizer, and the coordination between the baffle plate and the assisting roller makes it difficult for the fertilizer to move to the proper spreading area of the roller.

2.3.2 Upper deflector

The current surface and structural form of the upper deflector are both based on empirical values. Its surface refers to the departure angle and movement trajectory of the fertilizer with a good throwing distance. On this basis, the shape is determined using inverse fitting to fully correct and adjust the movement path of the fertilizer, further reduce its mechanical energy loss, and increase the effective throwing distance.

2.3.3 Side deflectors

According to the working principle and structural characteristics of the main throwing component, two types of deflectors, i.e., upper deflectors and side deflectors, are needed.

The side deflectors control the width of the fertilizer throwing flow through the constraint principle. To narrow the fertilizer flow, side deflectors are needed to further control the width to concentrate the flow, improve the resistance to air, and increase the effective throwing distance.

3 Relevant kinematic and dynamic analyses

This section focuses on fertilizer granules as microscopic particles. Through kinematic and dynamic analyses of the fertilizer granules detached from the scraper plate surface, the absolute velocity of the fertilizer granules at the moment of detachment can be determined. This velocity can be used to predict the throwing distance and investigate the relationship between the departure angle and the throw distance of fertilizer. This information will be

used for subsequent baffle plate optimization and shape formation of the deflector surface.

3.1 Analysis of the velocity at which the fertilizer granules detach from the surface of the scraper plate

The absolute velocity V_a at the moment when the fertilizer granules separate from the surface of the scraper plate can be defined by the following equation:

$$V_a = \sqrt{V_r^2 + V_e^2} \tag{1}$$

where, V_r is the relative velocity of the fertilizer granules when they detach from the surface of the scraper plate, m/s; and V_e is the velocity of fertilizer granules following the movement of the scraper plate when they detach from the surface of the scraper plate, m/s.

In this case, V_e is given by:

$$V_e = \omega R \tag{2}$$

where, ω is the disc angular velocity, rad/s; and R is the disc radius, m.

Before determining the absolute velocity V_a, the relative velocity V_r is first specified. A mechanical model of the fertilizer granules on the surface of the scraper plate is shown in Figure 3. The fertilizer granules are subjected to gravity G, which is decomposed into G_n and G_τ in Figure 3a and into $G_{\tau n}$ and $G_{\tau\tau}$ in Figure 3b, and subjected to the inertial centrifugal force F_c and Coriolis force F_k. Friction is not shown in the figure. Suppose that the landing point of fertilizer granules is M, the angle between the scraper plate and the vertical direction in the projection view at the time of the landing is γ, the fertilizer granules are thrown out after moving on the scraper plate up to S, the scraper plate rotates by an angle of ωt (t is the time of the fertilizer granules moving along the scraper plate, in s) during this time, and the sum of the two angles is ε. Under the resultant force F_r, the fertilizer granules move outward along the surface of the scraper plate. F_r can be expressed as follows:

$$F_r = F_c + G_{\tau\tau} - \mu(F_k + G_n + G_{\tau n}) \tag{3}$$

where, μ is the coefficient of friction.

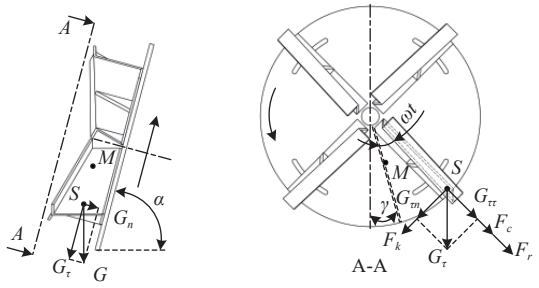

a. Front view b. A-A projection view

Figure 3 Establishment of mechanical model of fertilizer particles under the action of scraping fertilizer plate

(3) Considering the one-to-one correspondence of the force parameters in Equation (3), a differential form can be obtained as follows:

$$m\frac{d^2L}{dt^2} = mr\omega^2 + mg\sin\alpha\cos\varepsilon - \mu\left(2m\omega\frac{dL}{dt} + mg\cos\alpha + mg\sin\alpha\sin\varepsilon\right) \tag{4}$$

where, m is the mass of fertilizer granules, kg; g is the gravitational acceleration, m/s^2; and L is the path through which the fertilizer granules move along the surface of the scraper plate during the period from the time when the fertilizer granules fall on the scraper plate to the time when they are thrown out, m.

When the fertilizer granules move to point S, the distance r from the rotation axis of the disc is:

$$r = r_0 + L \tag{5}$$

where, r_0 is the distance between the position of the fertilizer granule just falling on the scraper plate and the rotation axis of the disc, m.

Substituting Equation (5) into Equation (4), a second-order linear differential equation is obtained as follows:

$$\frac{d^2L}{dt^2} + 2f_f\omega\frac{dL}{dt} - \omega^2 L = \omega^2 r_0 + g\sin\alpha\cos\varepsilon - f_f g\cos\alpha - f_f g\sin\alpha\sin\varepsilon \tag{6}$$

$$\begin{cases} L = \left[-\dfrac{U\sin\gamma}{2\omega(\lambda_1-\lambda_2)} - \dfrac{U\lambda_2\cos\gamma}{2\omega^2(\lambda_1-\lambda_2)} - \dfrac{K\lambda_2}{\omega^2(\lambda_1-\lambda_2)}\right]e^{\lambda_1 t} + \\ \quad \left[\dfrac{U\sin\gamma}{2\omega(\lambda_1-\lambda_2)} + \dfrac{U\lambda_2\cos\gamma}{2\omega^2(\lambda_1-\lambda_2)} + \dfrac{K\lambda_2}{\omega^2(\lambda_1-\lambda_2)} + \dfrac{U\sin\gamma}{2\omega^2} + \right. \\ \quad \left.\dfrac{K}{\omega^2}\right]e^{\lambda_2 t} - \dfrac{U\cos\varepsilon}{2\omega^2} - \dfrac{K}{\omega^2} \\ V_r = \dfrac{dL}{dt} = \left[-\dfrac{U\sin\gamma}{2\omega(\lambda_1-\lambda_2)} - \dfrac{U\lambda_2\cos\gamma}{2\omega^2(\lambda_1-\lambda_2)} - \dfrac{K\lambda_2}{\omega^2(\lambda_1-\lambda_2)}\right]\lambda_1 e^{\lambda_1 t} + \\ \quad \left[\dfrac{U\sin\gamma}{2\omega(\lambda_1-\lambda_2)} + \dfrac{U\lambda_2\cos\gamma}{2\omega^2(\lambda_1-\lambda_2)} + \dfrac{K\lambda_2}{\omega^2(\lambda_1-\lambda_2)} + \dfrac{U\sin\gamma}{2\omega^2} + \right. \\ \quad \left.\dfrac{K}{\omega^2}\right]\lambda_2 e^{\lambda_2 t} + \dfrac{U}{2\omega}\sin\varepsilon \\ \lambda_1 = \omega\left(\sqrt{f_f^2+1} - f_f\right),\ \lambda_2 = \omega\left(-\sqrt{f_f^2+1} - f_f\right) \\ K = \omega^2 r_0 - f_f g\cos\alpha,\ U = g\sin\alpha \end{cases} \tag{7}$$

By solving and transforming the above equation, the variation pattern of the velocity of the fertilizer granules moving along the surface of the scraper plate at any time t can be obtained, as shown in Equation (7). Substitution of the obtained V_r and Equation (2) into Equation (1) gives the absolute velocity V_a of the fertilizer granules that are detached from the scraper plate surface.

3.2 Relationship between the departure angle and throwing distance of fertilizer granules

The kinematic and dynamic model of fertilizer granules in the air is shown in Figure 4 (where δ is the departure angle). A Cartesian coordinate system O-XZ is established with O as the origin, the fertilizer throwing direction as the X-axis, and the upward direction perpendicular to the ground as the Z-axis. Only the influences of initial velocity, gravity, and air resistance are considered in the motion of fertilizer granules after they detach from the surface of the scraper plate. Since the scattering angle of the fertilizer has little effect on the content in this section, it is assumed that the fertilizer granules only move along the X–Z two-dimensional plane. The calculation formula for the air resistance f is shown in Equation (8). The actual fertilizer exists in both fine powder and coarse granular forms with an average diameter of 2 mm, and the granule model is simplified to a spherical shape. The

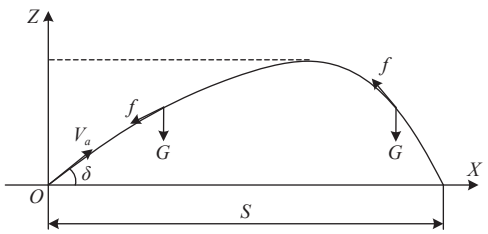

Figure 4 Kinematic and dynamic model of fertilizer granules in the XOZ plane

windward area S is the projected area of a fertilizer granule in the vertical direction, $\pi \cdot 10^{-6}$ m^2. The air resistance coefficient refers to the viscosity of wet soil (0.4 to 1.0) and is taken as the median value of 0.7.

$$f = \frac{1}{2} C \rho S V_a^2 \tag{8}$$

where, C is the air resistance coefficient, ρ is the air density (1.29 kg/m^3), and S is the windward area, m^2.

According to the motion model of fertilizer granules, the equations of motion are derived, as shown in Equation (9). They are implemented in MATLAB for numerical calculations of the throwing distance of the fertilizer under different departure angles. The throwing distance is used as an evaluation index to determine the departure angle of the fertilizer that yields the farthest (optimal) throwing distance under air resistance as well as the range of fertilizer departure angles that meet the technical specification of the throwing distance (throwing distance ≥10 m).

$$\begin{cases} \boldsymbol{P} = T_t \cdot \boldsymbol{V} \\ \boldsymbol{V} = \boldsymbol{V}_a + T_t \cdot \boldsymbol{a} \\ \boldsymbol{a} = \boldsymbol{a}_f + \boldsymbol{g} \end{cases} \tag{9}$$

where, $\boldsymbol{P}$ is the displacement of fertilizer granules at the current time, m; T_t is the simulation time interval, s; $\boldsymbol{V}$ is the velocity of fertilizer granules at the current time, m/s; $\boldsymbol{a}$ is the acceleration of fertilizer granules at the current time, m/s^2; and $\boldsymbol{a}_f$ is the air resistance acceleration, m/s^2.

During the simulation, the trajectory points of the fertilizer granules are generated every 0.05 s. The results are shown in Figure 5. Figure 5a shows the movement paths of the fertilizer with departure angles ranging from 20° to 45° (with intervals of 5°). As the departure angle at the time of fertilizer application gradually increased, the throwing distance tended to increase first and then decrease. The departure angle of the fertilizer that achieves the optimal (or farthest) throwing distance ranges between 26°-29°. The maximum and minimum departure angles that meet the 10 m throwing distance requirement range from 21° to 24° and from 31° to 34°, respectively. Next, the optimal departure angle, minimum departure angle, and maximum departure angle for the above three ranges are identified. The optimal departure angle is 27° (Figure 5b), and the minimum and maximum departure angles that meet the technical specifications of the 10 m throwing distance are 23° (Figure 5c) and 32° (Figure 5d), respectively.

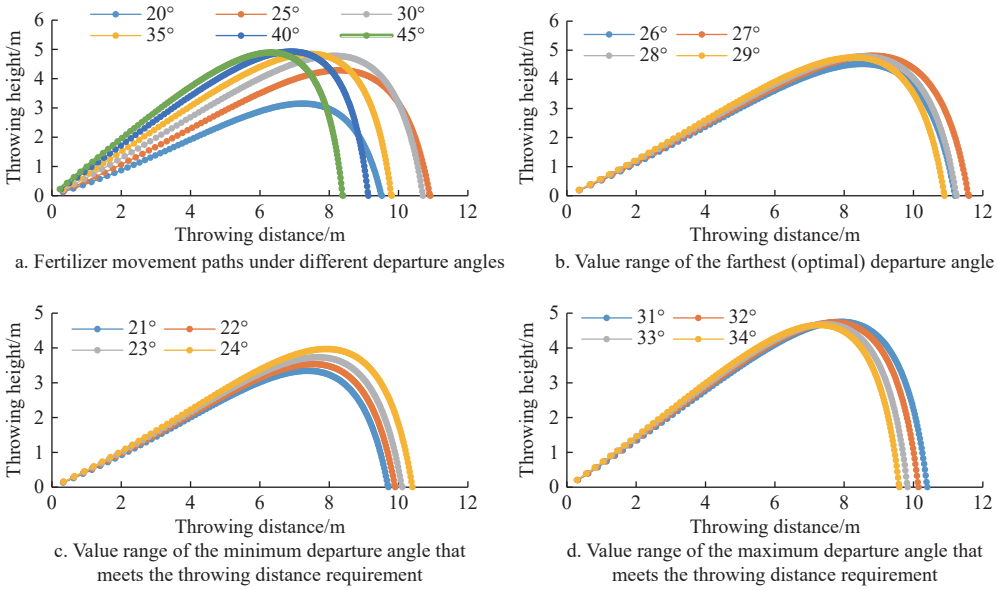

a. Fertilizer movement paths under different departure angles

b. Value range of the farthest (optimal) departure angle

c. Value range of the minimum departure angle that meets the throwing distance requirement

d. Value range of the maximum departure angle that meets the throwing distance requirement

Figure 5 Effect of the departure angle on the fertilizer movement path

4 Baffle plate analysis and optimization

4.1 Towing fertilizer

Due to the different areas where fertilizer falls on scraper plates, the velocity and movement patterns of fertilizer granules vary. The fertilizer that always follows the scraper plate and moves at the corresponding velocity is referred to as actively controlled fertilizer. Under the action of the scraper plate, this portion of the fertilizer can be smoothly thrown from the device. However, a small portion of the fertilizer accumulates at the end of the scraper plate and, during the rotation of the scraper plate, may break away from the control of the scraper plate and thus be in a dragged state. The portion of the fertilizer that gathers at the end of the scraper plate and eludes control at any time is referred to as the dragged fertilizer, as shown in Figure 6. Except for a small portion of the dragged fertilizer being thrown out from the side throw device along with the actively controlled fertilizer, a large portion of the fertilizer passed through the baffle plate to reach the throwing-assisting roller under the action of the scraper plate, and the remainder returned to the flexible cylinder cavity under the blocking effect of the baffle plate.

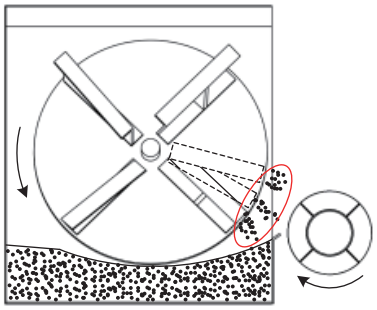

Figure 6 Schematic of towing fertilizer

4.2 Effect of the baffle plate structure on fertilizer movement and its optimization

4.2.1 Baffle plate height

As shown in Figure 7a, the vertical position of the upper edge of the baffle plate is roughly the same as that of the middle area of

the assisting roller. Most of the fertilizer thrown from the upper edge of the baffle plate collides with the assisting roller and is scattered to various positions, which may cause some interference in the normal spread of the fertilizer. However, it is difficult to adjust the position of the assisting roller due to installation space limitations. Therefore, to avoid obstructing the spreading of fertilizer by the assisting roller, the height of the baffle plate can be increased so that the trajectory of the fertilizer thrown out through the baffle plate is tangent to the outer circumference of the assisting roller, thereby fully allowing the assisting roller to perform secondary throwing of the fertilizer that falls nearby and thus avoiding the accumulation of fertilizer nearby.

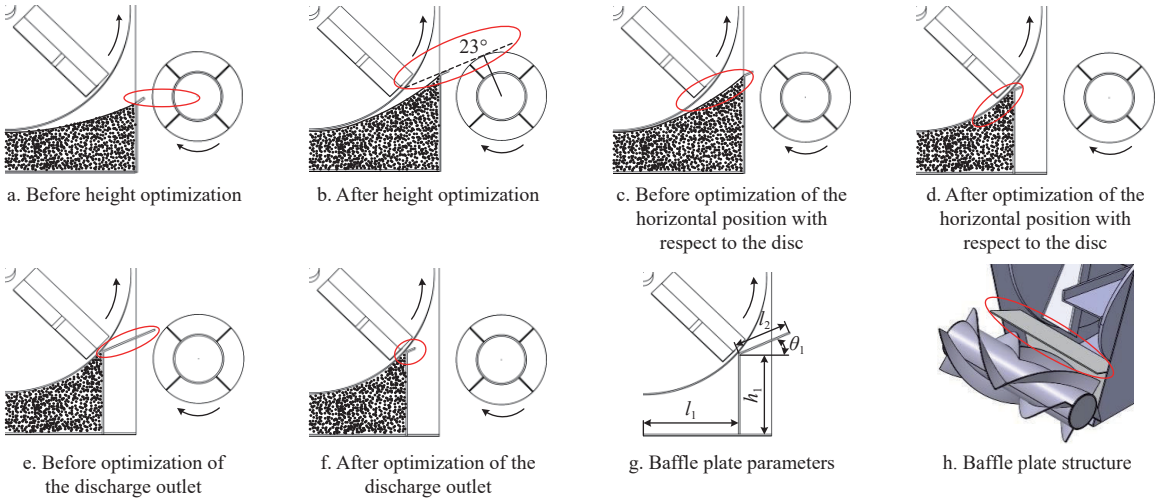

a. Before height optimization b. After height optimization c. Before optimization of the horizontal position with respect to the disc d. After optimization of the horizontal position with respect to the disc

e. Before optimization of the discharge outlet f. After optimization of the discharge outlet g. Baffle plate parameters h. Baffle plate structure

Figure 7 Optimization of baffle plate

As shown in Figure 7b, the height of the baffle plate can be increased by referring to the result obtained in Section 2.2 (the minimum departure angle of the fertilizer that meets the throwing requirement is 23°). Specifically, the height is raised to a line that is along the 23° direction and tangent to the outer circumference of the roller. After the baffle plate height increases, the fertilizer can, together with the actively controlled fertilizer, pass over the assisting roller above 23° at a higher initial velocity or fall onto the assisting roller but not drop nearby.

4.2.2 Horizontal positional relationship between the baffle plate and disc

After the height of the baffle plate is optimized, its role in the formation and limitation of the flexible cylinder cavity has not been fully realized. As shown in Figure 7c, there is still a large gap between the current flexible cylinder cavity and the envelope formed by one full rotation sweep of the scraper plate. When the scraper plate scrapes the fertilizer from the side of the flexible cylinder cavity away from the baffle plate to the gap area, the end of the scraper plate no longer touches the flexible cylinder cavity. As a result, the fertilizer at the end starts to fall off, and the velocity of the falling fertilizer (detached from the scraper plate) decreases significantly. The fertilizer cannot be replenished from the flexible cylinder cavity but can only be supplemented by the falling material flow. The amount of fertilizer in the area with the maximum linear velocity on the scraper plate decreases. Together, these two factors lead to a decrease in the proportion of fertilizer applied within a large throwing distance and an overall reduction in the effective throwing distance of fertilizer.

Therefore, the baffle plate is horizontally moved along the 23° dotted line to the outer edge of the disc, as shown in Figure 7d. At this time, the flexible cylinder cavity and the envelope are tightly fit, and there is no dragged fertilizer within the range of the flexible cylinder cavity. In addition to receiving the falling material flow, the scraper plate can also scrape the fertilizer in the flexible cylinder cavity, which is scraped in the high-velocity area at the end until being thrown out, demonstrating a good spreading effect.

4.2.3 Baffle plate discharge outlet

After the horizontal positional relationship between the baffle plate and the disc is optimized, it is difficult for the fertilizer to be transferred via the baffle plate to the effective throwing area of the assisting roller, as shown in Figure 7e. Therefore, for better fertilizer transfer, a discharge outlet is added above the baffle plate, as shown in Figure 7f. The 23° inclined surface serves as a transfer platform. When the scraper plate rotates to the spreading moment, the dragged fertilizer falling from the end can fall onto the inclined surface of the discharge outlet, and the portion of fertilizer with high kinetic energy is transferred to the assisting roller by the inclined surface. The combined action of the two ensures that there is almost no fertilizer falling between the device and the assisting roller. The inclined surface also acts as a buffer platform, and fertilizer with low kinetic energy is retained on the inclined surface and pushed out by subsequent fertilizer or slides back to the main area of the cylinder cavity to be scattered by the secondary action of the scraper plate. The discharge outlet is shown in Figure 7f.

At this point, the optimization of the baffle plate structure is complete, and its main parameters are shown in Figure 7g. Here, based on the previous analysis, θ_1 is 23°, h_1 is 162 mm, and l_1 and l_2 are 195 mm and 110 mm, respectively. The optimized baffle plate is shown in Figure 7h.

4.3 Comparison of the baffle plate optimization simulation results

To examine the role of the improved baffle plate in transferring fertilizer and limiting the flexible cylinder cavity structure, numerical simulations are performed using EDEM, as shown in Figure 8. Figure 8a shows the flexible cylinder cavity structure generated before baffle plate optimization under baffle plate blockage and scraper plate scraping. Due to the low baffle plate height, there is a large gap between the flexible cylinder cavity and the envelope obtained by sweeping the scraper plate in one rotation. Figure 8b shows that after baffle plate improvement, the flexible cylinder cavity generated under the combined action of the baffle plate and the scraper plate fits perfectly with the envelope, which is

consistent with the theoretical analysis results. Figure 8c shows a side view of the fertilizer spreading through the side throw device before the baffle plate improvement. There is leakage in the gap between the baffle plate and the assisting roller, causing fertilizer accumulation and waste in nearby areas. In addition, fertilizer cannot be transferred to the effective throwing area of the assisting roller via the baffle plate, and the assisting roller hinders fertilizer spreading. Figure 8d shows the results of fertilizer spreading through the side throw device after baffle plate improvement. In this case, material leakage disappears, the fertilizer is transferred through the baffle plate discharge outlet to the effective spreading area of the assisting roller, and the baffle plate can limit the minimum fertilizer departure angle to 23°.

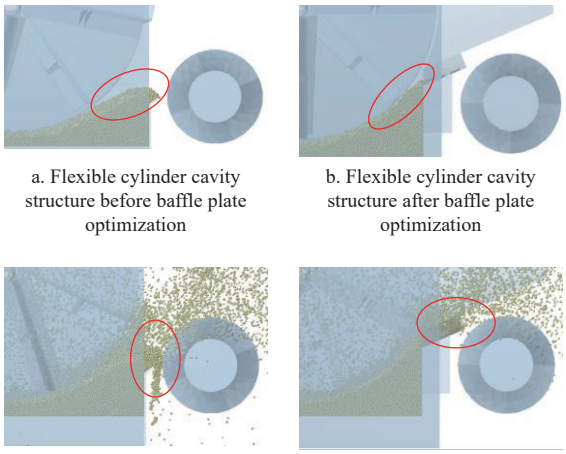

a. Flexible cylinder cavity structure before baffle plate optimization

b. Flexible cylinder cavity structure after baffle plate optimization

c. Fertilizer discharge before baffle plate optimization

d. Fertilizer discharge after baffle plate optimization

Figure 8 Comparison of simulation results before and after baffle optimization

5 Structural analysis and design of deflectors

5.1 Curved surface formation of the upper deflector

Based on the earlier analysis, the optimal departure angle of the fertilizer that meets the throwing distance requirement is 27°. Therefore, the diversion angle at the end of the deflector can be set to 27° so that the fertilizer with a large departure angle can be corrected by the upper deflector and then thrown at 27°, moving together with the fertilizer with a good throwing distance to reduce the mechanical energy loss. Furthermore, because the maximum departure angle that meets the throwing distance requirement is 32°, when the departure angle is greater than 32°, the fertilizer granules have a high velocity, a large throwing angle, and a steep trajectory. Forcible correction of the alignment to 27° would cause significant mechanical energy loss. Therefore, a two-stage correction of fertilizer movement paths is adopted using two curved surfaces with different curvatures. Eventually, the fertilizer granules thrown at angles greater than 27° are adjusted to an angle of 27° to the ground, and many fertilizer granules are thrown together. In addition, due to their adhesive properties, these materials can move together, increasing their resistance to wind and further reducing their mechanical energy loss.

The surface structure and parameters of the upper deflector are shown in Figure 9. Figure 9a shows the front view. The length of the correction area is jointly determined by the action position of the fertilizer granules and the installation location; l_3 is set to 420 mm. Figure 9b shows the right view of the deflector structure, with the main parameters indicated in the figure. Its construction line is the splicing of an arc structure with a certain curvature and a planar structure; l_4 and l_5 are both 100 mm, R_0 is 200 mm, the angle θ_2 between the tangent direction at the junction of the arc and the curved surface with the horizontal line is set to 32°, the angle between the tangent direction at the outlet above the planar structure and the horizontal line is determined according to the optimal departure angle during the movement of fertilizer granules, and θ_3 is set to 27°.

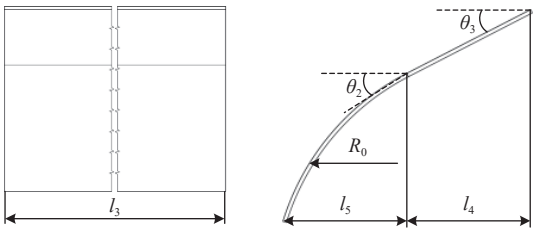

a. Front view b. Left view

Figure 9 Structure and parameters of upper guide plate

Before the upper deflector is installed, its spatial relationship with the main spreading device (inclined opposing discs with a scraper plate) needs to be clarified. The installation of the upper deflector is shown in Figure 10. The deflector is placed at the center between the two discs (Figure 10a). In Figure 10b, in the horizontal direction, the distance l_6 between the midpoint of the curve at the lower end of the upper deflector and the rotation center of the disc is 260 mm; in the vertical direction, the upper deflector needs to be suspended from the upper beam during installation, and the upper deflector must not interfere with the rotating scraper plate during operation. The maximum envelope formed by the sweeping of the scraper plate in one rotation is shown in Figure 10b. Hence, the distance l_7 between the upper deflector and the disc in the vertical direction is 134 mm.

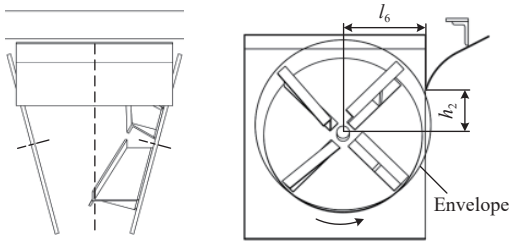

a. Front view b. Right view

Figure 10 Spatial position relationship between upper guide plate and disc

The structure of the upper deflector is shown in Figure 11. The blocking structure in Figure 11a is used to block the fertilizer that is beyond the control range of the upper deflector, so this part of the fertilizer can be returned to the side throw device for re-spreading. The hangers in Figure 11b are used to connect the upper deflector and the upper crossbeam.

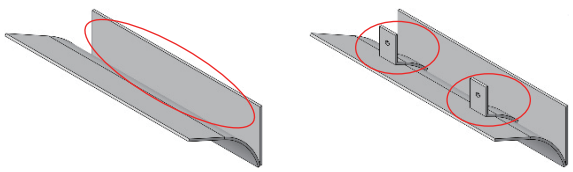

a. Blocking structure b. Hangers

Figure 11 Upper guide plate structure

5.2 Analysis and design of side deflectors

5.2.1 Correction analysis of fertilizer spreading with large scattering angles

During fertilizer spreading, in a flow with small scattering

angles, most of the fertilizer granules move together, while in a flow with large scattering angles, individual fertilizer granules or small clusters of fertilizer granules move independently. The former, relative to the latter, enhances the overall ability to resist air resistance and reduces the mechanical energy dissipated by the fertilizer due to movement to both sides, and this portion of mechanical energy can be used for the fertilizer to travel a greater distance along the throwing direction. Therefore, to reduce mechanical energy dissipation, it is necessary to install side deflectors on the device to limit fertilizer spreading with large scattering angles.

When designing side deflectors, in addition to allowing them to correct the divergent throwing flow, consideration should also be given to ensuring that these structures do not affect the fertilizer moving in an oblique upward direction. To this end, the centerline of the cavity formed by the deflectors on both sides is inclined upward at 27° (the fertilizer throwing distance is the farthest when the fertilizer throwing angle is 27°). In this spatial state, the effects of the arc structure on the deflection of the side deflectors and the correction of the fertilizer throwing flow were analyzed.

As shown in Figure 12, a Cartesian coordinate system *XOY* is established with *O* as the origin, the fertilizer spreading direction as the *X*-axis, and the movement direction of the implement as the *Y*-axis. In Figures 12a and 12b, the black trajectory lines schematically represent the movement path of fertilizer when no side deflector is installed. After the fertilizer separates from the surface of the scraper plate, some of it disperses outward along the *Y*-axis direction. The red trajectory lines schematically represent the corrective effect of side deflectors on the movement path of the fertilizer. Even after the fertilizer separates from the surface of the scraper plate, it still disperses outward along the *Y*-axis, but under the corrective effect of side deflectors, the movement path of the fertilizer changes from a divergent state to an inward concentration along the *Y*-axis. The fertilizer throwing flow changes from a divergent state to a concentrated state. The ability of fertilizer to overcome air resistance during spreading is enhanced, and some of the mechanical energy acting on fertilizer is saved and used for long-distance movement.

When the affected fertilizer separates from the surface of the scraper plate but has not reached the side deflectors, this part of the fertilizer can be divided into three cases based on its departure angle, i.e., greater than, equal to, and less than 27°. As shown in Figure 13, a Cartesian coordinate system *O-XZ* is established with *O* as the origin, the direction of fertilizer spreading as the *X*-axis, and the vertical upward direction perpendicular to the ground as the *Z*-axis. Figures 13a-13c schematically depict the corrective effect of side deflectors when the departure angle of the fertilizer is greater than, equal to, and less than 27°, respectively. The black trajectory represents the situation without side deflectors installed. The movement paths of the fertilizer on the *XOZ* plane are quite different due to the different departure angles. The red trajectory represents the situation after the side deflectors are installed. Under the corrective effect of side deflectors, the movement path of the affected fertilizer changes. When the departure angle is greater than 27°, the fertilizer is deflected upward along the 27° direction, corrected to the flow with the farthest throwing distance, moving together with this throwing flow, providing better resistance to air, and reducing mechanical energy loss due to upward movement along the *Z*-axis, converting the ascent distance into forward distance along the throwing direction. When the departure angle of the fertilizer is approximately 27°, although the side deflectors do not change the movement path or trajectory, they can prevent the influence of lateral airflow along the *Y*-axis direction in the working area of the side deflectors. When the departure angle of the fertilizer is less than 27°, the arc-shaped structure at the lower part of the side deflectors acts as a support and can utilize the remaining mechanical energy of the fertilizer to correct its direction along the flow direction with the farthest throwing distance.

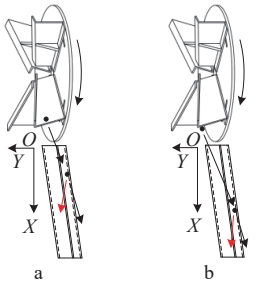

Figure 12 Movement path change of the affected fertilizer in the *XOY* plane

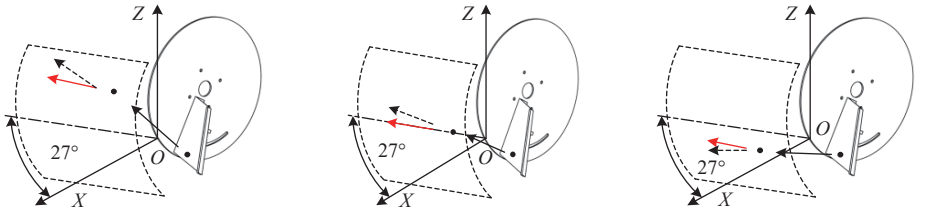

a. Departure angle >30° (with side deflector installed) b. Departure angle =30° (with side deflector installed) c. Departure angle <30° (with side deflector installed)

Figure 13 Movement path change of the affected fertilizer in the *XOZ* plane

5.2.2 Structural design of side deflectors

Based on the theoretical solution and the analysis of the working principle of side deflectors, it is concluded that the fertilizer throwing distance is the greatest when the fertilizer departure angle is 27°. To prevent the side deflector structure from interfering with the oblique upward movement of the fertilizer, it is designed as an arc structure with an oblique upward angle of 27°. As shown in Figure 14a, when observed from the angle of the normal line of the throwing trajectory of fertilizer with a departure angle of 27°, this arc structure can optimize the throwing path during fertilizer spreading, minimizing the mechanical energy loss of the fertilizer during the spreading process. Meanwhile, to prevent the scraper plate from obstructing the spreading of the fertilizer, it is placed roughly in the same plane as the disc. After the angle is set, interference between the side deflectors and other components, namely, the disc and the assisting roller, should be avoided, as shown in Figure 14b. As shown in Figure 14c, the side deflectors are installed by means of the upper

deflector, and the two deflectors are connected to the cross beam. After installation and fixation, there is no gap between the upper deflector and side deflectors, preventing the fertilizer from splashing outward. At the same time, the two deflectors work together to reduce the size of the discharge outlet. As a result, the fertilizer can be directly corrected and adjusted by the two deflectors after being thrown out, which is more conducive to concentrating the flow of applied fertilizer.

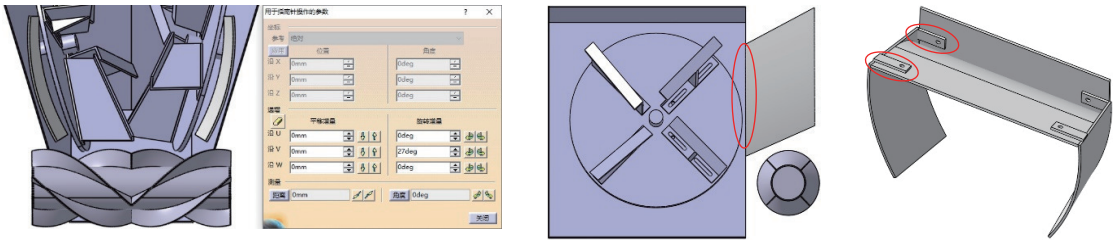

a. Construction line normal view b. Positional relationship with other c. Installation of side deflectors

Figure 14 Structure of the side guide plate

6 Technology integration and virtual simulation

6.1 Simulation model establishment

In this study, stationary spreading[6] is considered in the simulation to examine the correction and adjustment effect of each auxiliary mechanism component on fertilizer throwing flow. Before the simulation, a side throw device model is created. Without affecting the simulation results, structures that are not practically significant for virtual simulation are simplified. The simplified side throw device is shown in Figure 15a. To facilitate the observation of fertilizer spreading, a ground model for stationary spreading (Figure 15b) is created, with dimensions of 15 000 mm (spreading direction)×3000 mm×20 mm.

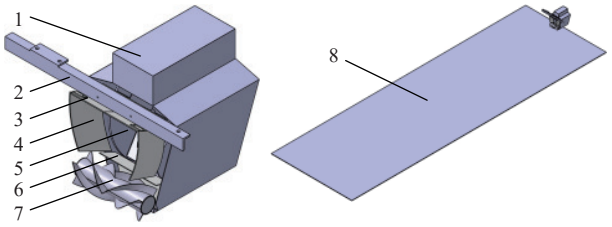

a. Structure of a simplified side throw device b. Ground model

1. Hopper; 2. Crossbeam (used to indicate the assembly relationship and can be deleted in the simulation); 3. Upper deflector; 4. Side deflector; 5. Fertilizer spreading disc with a scraper plate; 6. Baffle plate; 7. Assisting roller; 8. Ground

Figure 15 Simulation model of the side throw device

6.2 Simulation parameter setting

In the simulation, the fertilizer granules are simplified as spherical models. The model radius is set to 2 mm based on the actual average granule size, and the granule sizes are randomly distributed. The parameters for the fertilizer, steel, and soil as well as their contact with each other[12-14] are shown in Table 2. Due to the moisture content in the fertilizer and soil, significant adhesion and aggregation occur. Therefore, the Hertz–Mindlin model and the JKR model[15,16] are used as contact models between fertilizer granules and between the fertilizer and soil. The Hertz–Mindlin (no-slip) model[17,18] is used between the fertilizer granules and the side throw device. The particle factory is set up in the hopper, with the type set to dynamic and a granule generation rate of 15 kg/s. The total simulation time is 14 s, with a feeding duration of 10 s[19]. After feeding, the remaining 4 s allow the fertilizer to fall freely until it reaches the ground. The disc rotates at 700 r/min, while the roller rotates at 2238 r/min within a rotation time of 0-10 s. The time step is fixed at 20% of the Rayleigh time step, and the data are recorded every 0.02 s[20,21].

6.3 Simulation process and evaluation index determination method

6.3.1 Presimulation preparation and simulation process

In order to maximize the reproduction of the real spreading effect, before spreading the need for the simulation model to add a flexible barrel cavity, flexible barrel cavity by the natural accumulation of fertilizer particles constitute a simulation before the introduction of the side-throwing device model for the formation of flexible barrel cavity, as shown in Figure 16a, according to the simulation parameter settings to run the simulation, the bottom of the observation of the side-throwing device until the formation of a complete flexible barrel cavity, the formation of a flexible barrel cavity of the model is saved as a new simulation model time reset to 0s, the flexible cylinder cavity generation process is shown in Figure 16b. In addition, to prevent fertilizer granules from continuing to roll after landing, soil particles are added to the ground model, and the simulation environment is shown in Figure 16c. The simulation effect of stationary spreading is shown in Figure 17.

Table 2 Basic parameters of the EDEM simulation

Item	Parameter	Value
Fertilizer	Poisson's ratio	0.4
	Shear modulus/Pa	2×10^{6}
	Density/kg·m^{-3}	800
	Surface energy/J·m^{-2}	0.045
Steel	Poisson's ratio	0.31
	Shear modulus/Pa	7×10^{10}
	Density/kg·m^{-3}	7900
	Surface energy/J·m^{-2}	0.0225
Soil	Poisson's ratio	0.3
	Shear modulus/Pa	5×10^{7}
	Density/kg·m^{-3}	2600
	Surface energy/J·m^{-2}	0
Fertilizer–fertilizer	Recovery coefficient	0.6
	Static friction coefficient	0.65
	Dynamic friction coefficient	0.1
Fertilizer–steel	Recovery coefficient	0.6
	Static friction coefficient	0.7
	Dynamic friction coefficient	0.11
Fertilizer–soil	Recovery coefficient	0.4
	Static friction coefficient	0.66
	Dynamic friction coefficient	0.18

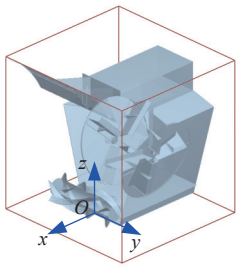

a. EDEM model used to generate the flexible cylinder cavity

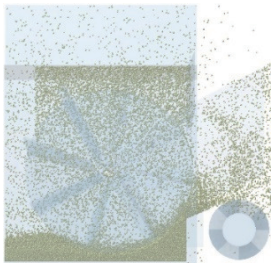

b. Process of generating the flexible cylinder cavity

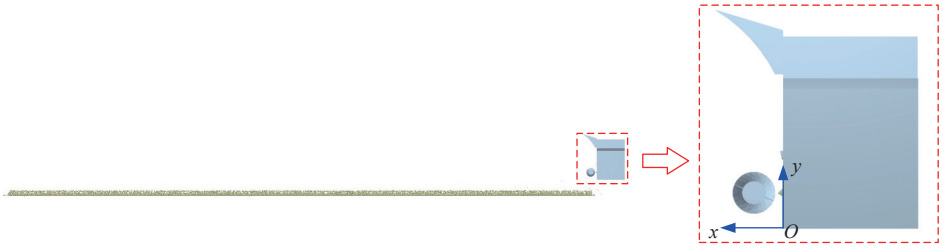

c. Addition of soil particles to the EDEM ground model

Figure 16 EDEM model preparation before simulation

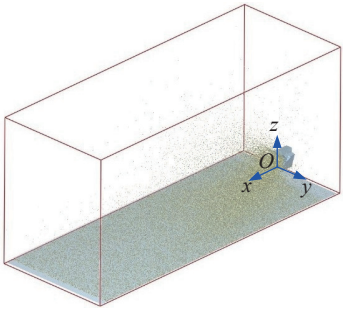

Figure 17 Fixed-point form scattering simulation process

6.3.2 Methods for determining evaluation indices

To evaluate the overall correction and adjustment effects of the auxiliary mechanisms on the fertilizer throwing flow, two evaluation indices are set, namely, the uniformity coefficient of variation and the material flow scattering angle. The throwing simulation process is repeated three times, and three sets of measured data were averaged to observe the change rule.

(1) Uniformity coefficient of variation

According to the environmental protection requirements and test methods for fertilizer spreaders[22], the uniformity coefficient of variation of fertilizer should be less than 30%. Before determining the uniformity coefficient of variation, multiple collection boxes with dimensions of 500 mm×500 mm×100 mm are set up according to the spreading coverage area, and the mass of fertilizer in the collection box that meets the requirements is weighed. The uniformity coefficient of variation is calculated using Equation (10). The stationary scattering method involves continuously stacking the throwing flow on the ground to form a coverage area. Due to the scattering phenomenon of the material flow, there is a certain gap between the width at the starting end and the width at the finishing end. Using conventional collection boxes can lead to deviations in the determination of indicators. Therefore, a method that is different from spreading in conventional mobile operation is adopted. The collection boxes are arranged along the spreading direction, as shown in Figure 18.

The size of each collection box is 5000 mm×500 mm×100 mm (the length of the collection box is set according to the maximum spreading width, and the width and height remain unchanged). The mass of fertilizer in each collection box is measured, and the uniformity coefficient of variation is calculated using the following equation:

$$\begin{cases} CV\left(100\%\right)=\dfrac{S}{\bar{x}}100 \\ S=\sqrt{\dfrac{1}{n-1}\sum_{i=1}^{n}(x_i-\bar{x})^2} \\ \bar{x}=\dfrac{1}{n}\sum_{i=1}^{n}x_i \end{cases} \tag{10}$$

where, CV is the uniformity coefficient of variation, %; S is the standard deviation; $\bar{x}$ is the mean amount of fertilizer applied, kg; x_i is the amount of fertilizer in the fertilizer collection box after overlapping, kg; and n is the number of fertilizer collection boxes in the spreading area.

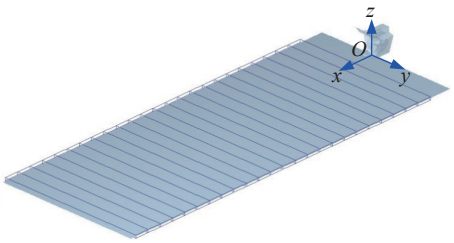

Figure 18 Determination of dispersion uniformity in fixed-point form

(2) Scattering angle

During stationary spreading, the throwing flow completely lands to form a fertilizer coverage area. The angle between the two sides of the coverage area, that is, the scattering angle, is measured.

6.4 Comparison of the optimization results of the auxiliary mechanisms

Figure 19 compares the results of stationary throwing by the side throw device before and after auxiliary mechanism optimization. The optimized auxiliary mechanisms, on the basis of a good main throwing flow, work better in coordination with the main throwing component to correct the overall material flow. From the intuitive perspective of fertilizer coverage on the ground, the throwing flow of fertilizer is more concentrated and has better uniformity.

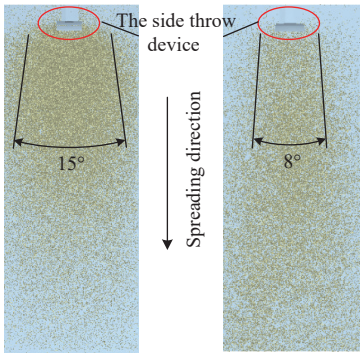

a. Before optimization b. After optimization

Figure 19 Comparison of the scattering effect before and after optimization of the auxiliary mechanism

The measurements show that after optimization of the auxiliary mechanisms, the uniformity coefficient of variation decreases from 28.76% to 21.55%, and the scattering angle decreases from 15° to 8°, as listed in Table 3. The simulation results show that the optimization effect of the auxiliary mechanisms is satisfactory and can effectively improve the spreading performance of the side throw device.

Table 3 Comparison of the simulation results before and after optimization of the auxiliary mechanism

Types of auxiliary institutions	Uniformity coefficient of variation/%	Scattering angle/(°)
Before optimization	28.76	15
After optimization	21.55	8

7 Experimental apparatus design and testing

7.1 Experimental apparatus and materials

The experiments were conducted on October 1 to 2, 2023, at Northeast Agricultural University. The weather was clear and sunny, with a temperature ranging from 8°C to 23°C and a wind speed ranging from 2 to 4 km/h. As shown in Figure 20, a side throw device with optimized auxiliary mechanisms included inclined opposing discs with fertilizer scraper plates, assisting rollers, and auxiliary mechanisms. During the experiments, the discs acted as the main throwing component with a rotation speed of 700 r/min, and the assisting roller was the auxiliary throwing component with a rotation speed of 2238 r/min. The feeding rate was 15 kg/s, and the spreading time was 10 s.

a. Front view b. Axonometric view

Figure 20 Side-throwing device with optimized auxiliary mechanism

According to the current standards for organic fertilizer in the Chinese domestic industry[23], commercial ecological organic fertilizer from Harbin Yilirong Agricultural Technology Co., Ltd., was chosen as the experimental material[5].

7.2 Experimental methods

There were two types of side throw devices in the experiments: one with auxiliary mechanisms installed before optimization and the other with auxiliary mechanisms installed after optimization. A comparison between the two was made in terms of spreading effects and parameters to examine the optimization effects of the subsidiary mechanisms. Furthermore, spreading was conducted in two forms: stationary and mobile operations. Through stationary spreading, the morphology of fertilizer flow, the angle between the throwing flow and the horizontal plane, the scattering angle, and the effective throwing distance of the side throw device before and after optimization were observed. Through mobile operations, the overall spreading coverage area formed by the continuous landing and superposition of the throwing flow was observed. The uniformity coefficient of variation was measured. The size of the discharge opening to be opened was calculated according to the set feeding quantity, and the feeding rake chain was opened to complete the feeding and spreading. The methods used to measure the scattering angle and effective throwing distance are shown in Figure 21a. The fertilizer collection boxes were used to measure the uniformity coefficient of variation. As shown in Figure 21b, after fertilizer spreading was completed, the mass of fertilizer in each collection bin was weighed using an electronic scale, and the uniformity coefficient of variation was calculated. Each test was repeated three times, and three sets of measured data were averaged to observe the change rule.

a. Distance measurement b. Fertilizer collection boxes

Figure 21 Parameter determination methods

7.3 Experimental results and analysis

Figure 22 compares the spreading effects of the side throw device before (Figures 22a-22c) and after (Figures 22d-22f) auxiliary mechanism optimization. Comparing Figures 22a and 22d from the perspective of stationary spreading, after the optimization of the auxiliary mechanisms, the range of the included angle of the throwing flow decreased, the throwing flow became more concentrated, the angle between the main throwing flow and the horizontal plane decreased, and the effective throwing distance increased. Based on these observations, the upper deflector and the baffle plate had a good correction and adjustment effect on the fertilizer with overly large or small departure angles, which conserved the extra mechanical energy that would otherwise have been required for the fertilizer to overcome the air resistance upward; the saved mechanical energy was used for long-distance movement in the spreading direction. Comparing Figures 22b and e from the perspective of stationary spreading, after the ancillary mechanisms were optimized, the scattering angle decreased, resulting in a narrower throwing flow and an increase in the effective throwing distance. The installation of side deflectors reduced the amount of fertilizer spreading to the two sides, allowing the mechanical energy otherwise supporting the movement to the two sides to be used for long-distance movement along the spreading direction, thus increasing the overall spreading distance. Comparing the spreading effects of the mobile operation between Figures 22c and 22f, the overall throwing distance is farther, and the spreading uniformity is better. The side throw device spreading results before and after the optimization of the auxiliary mechanism are compared in Table 4.

a. Stationary spreading before optimization (angle between throwing flow and horizontal plane, effective throwing distance)

b. Stationary spreading before optimization (scattering angle)

c. Spreading effect of mobile operation before optimization

d. Stationary spreading after optimization (angle between throwing flow and horizontal plane, effective throwing distance)

e. Stationary spreading after optimization (scattering angle)

f. Spreading effect of mobile operation after optimization

Figure 22 Comparison of the throwing effect of the side-throwing device before and after optimization of the auxiliary mechanism

Table 4 Comparison of the scattering results of the side-throwing device before and after optimization of the auxiliary mechanism

Types of auxiliary mechanisms	Angle between main throwing flow and horizontal plane/(°)	Maximum angle between the throwing flow and horizontal plane/(°)	Minimum angle between the throwing flow and horizontal plane/(°)	Scattering angle/(°)	Effective throwing distance/m	Uniformity coefficient of variation/%
Before optimization	34	45	18	12	10.1	25.95
After optimization	27	32	23	4	11.2	19.21

Comparing the results of the virtual simulation and prototype test, the coefficient of variation of uniformity decreases from 28.76% to 21.55% before and after optimization in virtual simulation, and from 25.95% to 19.21% before and after optimization in the prototype test; the scattering angle decreases from 15° to 8° before and after optimization in the virtual simulation, and from 12° to 4° before and after optimization in the prototype test. The coefficient of variation of uniformity decreases by 7.21% and the scattering angle decreases by 7° before and after optimization in the virtual simulation, and the coefficient of variation of uniformity decreases by 6.74% and the scattering angle decreases by 8° before and after optimization in the prototype test. It can be seen that due to the vibration of the machine, the ambient wind speed, the particle crushing, and the adhesion effect, etc., the results of the prototype test differ from the results of the virtual simulation to a certain extent. However, the virtual simulation and the prototype test show the optimization effect and the trend is consistent, indicating that the optimization scheme provides feasibility and effectiveness.

8 Conclusions

(1) Based on relevant kinematic and dynamic analyses as well as MATLAB numerical calculations, the departure angle of fertilizer with the longest throwing distance is 27°, and the maximum and minimum departure angles of fertilizer that meet the requirements of the target 10 m throwing distance are 32° and 23°, respectively.

(2) A baffle plate is used to adjust the fertilizer departure angle from 18° to 23°, and the horizontal distance between the center points of the two main throwing discs is set to 195 mm. The flexible cylinder cavity is well formed, there is no material leakage between the baffle plate and the assisting roller, and the dragged fertilizer can be smoothly transferred to the effective feeding area of the assisting roller through the material discharge outlet structure.

(3) The upper deflector uses a two-stage variable curvature arc structure to correct the angle between the main throwing flow and the horizontal plane to 32° first and then to 27°. The large scattering angle of the fertilizer can be corrected using side deflectors placed on both sides of the disc. By utilizing its inclined arc structure, the main throwing flow can be further corrected to 27°. The combined effect of the two stages effectively concentrates the main throwing flow.

(4) The included angle range of the throwing flow is adjusted from 18°-45° to 23°-32° to coordinate with the optimization of other auxiliary mechanisms; the uniformity coefficient of variation of the throwing flow decreases from 25.95% to 19.21%, the effective throwing distance increases from 10.1 to 11.2 m, and the scattering angle is reduced from 12° to 4°, effectively enhancing the spreading performance of the side throw device.

Acknowledgements

The authors acknowledge that this work was financially supported by the “Suqian Talent” Xiongying Program for Educational Innovation Talents Project (Grant No. SQXY202431) and the Heilongjiang Province First-Level Leading Talents Reserve Leader Foundation ([2017] 487).

The authors are grateful to the editors and anonymous reviewers for providing helpful suggestions to improve the quality of this work.

[References]

[1] Wang H X, Xu J L, Liu X J, Zhang D, Li L W, Li W, et al. Effects of long-term application of organic fertilizer on improving organic matter content and retarding acidity in red soil from China. Soil and Tillage Research,

2019; 195: 104382.
[2] Zhang H, Xu M, Zhang F. Long-term effects of manure application on grain yield under different cropping systems and ecological conditions in China. The Journal of Agricultural Science, 2009; 147(1): 31–42.
[3] Zhang J, Xu N T, Meng Q F, Jiang B W. Effect of years of manure fertilizer application on soil organic carbon component, its source and corn yield. Transactions of the CSAE, 2019; 35(2): 107–113.
[4] Du W Y, Tang S, Wang H. The status of organic fertilizer industry and organic fertilizer resources in China. Soil and Fertilizer Sciences in China, 2020; 3: 210–219.
[5] Liu H X, Du C L, Yin L W, Zhang G F. Shooting flow shape and control of organic fertilizer side throwing on inclined opposite discs. Transactions of the CSAM, 2022; 53(1): 168–177.
[6] Liu H X, Zhao Y J, Xie Y T, Zhang Y M, Shang J J. Design and experiment of spiral blades auxiliary roller of organic fertilizer side throwing device. Transactions of the CSAM, 2023; 54(4): 107–119.
[7] Zhang G Z, Wang Y, Liu H P, Ji C, Hou Q X, Zhou Y. Design and experiments of the centrifugal side throwing fertilizer spreader for lotus root fields. Transactions of the CSAE, 2021; 37(19): 37–47.
[8] Fan C, He R, Shi Y, He L. Structure and operation mode of centrifugal side-throwing organic fertilizer spreader for greenhouses. Powder Technology, 2024; 438: 119457.
[9] Xu B, Cui Q L. Improvement design and simulation analysis on centrifugal disc organic fertilizer spreader. INMATEH-Agricultural Engineering, 2023; 70(2). doi: 10.35633/inmateh-70-32
[10] Bulgakov V, Adamchuk O, Pascuzzi S, Santoro F, Olt J. Research into engineering and operation parameters of mineral fertiliser application machine with new fertiliser spreading tools. Agronomy Research, 2021; doi: 10.15159/AR.21.040
[11] Zhou Z, Zhao J G, Yin B Z, Li L X, Jia H T, Zhang B C, et al. Optimized design and experiment of a spatially stratified proportional fertilizer application device for summer corn. ACS omega, 2022; 7(24). doi: 10.1021/acsomega.2c01273
[12] Liu H X, Wang C, Wang J X, Fu L L. Design and experiment study on portable in-vehicle device of farmyard manure collecting. Journal of Northeast Agricultural University, 2017; 48(9): 59–71, 96.
[13] Peng C W, Xu D J, He X, Tang Y H, Sun S L. Parameter calibration of discrete element simulation model for pig manure organic fertilizer treated with *Hermetia illucen*. Transactions of the CSAE, 2020; 36(17): 212–218.
[14] Yuan Q C, Xu L M, Xing J J, Duan Z Z, Ma S, Yu C C, et al. Parameter calibration of discrete element model of organic fertilizer particles for mechanical fertilization. Transactions of the CSAE, 2018; 34(18): 21–27.
[15] Zeng Z W, Ma X, Cao X L, Li Z H, Wang X C. Critical review of applications of discrete element method in agricultural engineering. Transactions of the CSAM, 2021; 52(4): 1–20.
[16] Tan H C, Xu L M, Ma S, Niu C, Yan C G, Shen C C. Design and experiment of scraper organic fertilizer strip spreading and rotary tillage mixed fertilizer applicator. Transactions of the CSAM, 2022; 53(11): 163–175.
[17] Liao Y T, Gao L P, Liao Q X, Zhang Q S, Liu L C, Fu Y K. Design and test of side deep fertilizing device of combined precision rapeseed seeder. Transactions of the CSAM, 2020; 51(2): 65–75.
[18] Yang W W, Fang L Y, Luo X W, Li H, Ye Y Q, Liang Z H. Experimental study of the effects of discharge port parameters on the fertilizing performance for fertilizer distribution apparatus with screw. Transactions of the CSAE, 2020; 36(17): 1–8.
[19] Dun G Q, Yu C L, Guo Y L, Ji W Y, Islam k R, Du J X. Design and experiment of double-gear type fertilizer apparatus. Transactions of the CSAM, 2020; 51(3): 87–96.
[20] Hou Q F, Dong K J, Yu A B. DEM study of the flow of cohesive particles in a screw feeder. Powder Technology, 2014; 256: 529–539.
[21] Kretz D, Callau-Monje S, Hitschler M, Hien A, Raedle M, Hesser J. Discrete element method (DEM) simulation and validation of a screw feeder system. Powder Technology, 2016; 287: 131–138.
[22] Standardization Administration of China. Agricultural machinery - manure spreaders - environmental protection - requirements and test methods: GB/T 25401-2010. Beijing: China Standard Publishing House, 2010. (in Chinese)
[23] Agricultural Technology Extending Service Center of China. Rule of rational fertilization: NY/T 496-2010. Beijing: China Standard Publishing House, 2010. (in Chinese)